

SYNTHESIS OF HIGH PURITY MAGNESIA MgO FROM ALGERIAN DOLOMITE ORE

C. Bouchekrit ^{a, b}, M. Kolli ^{a, b, *}, M. Altiner ^c, R. Doufnoune ^{a, d}

^a Ferhat Abbas Setif 1 University, Emergent Materials Research Unit, Setif, Algeria

^b Ferhat Abbas Setif 1 University, Optics and Precision Mechanics Institute, Setif, Algeria

^c Çukurova University, Mining Engineering Department, Adana, Türkiye

^d Ferhat Abbas Setif 1 University, Faculty of Technology, Setif, Algeria

(Received 06 April 2022; Accepted 27 December 2022)

Abstract

A nanometric $Mg(OH)_2$ and MgO particles with high purity were successfully synthesized from Algerian dolomite via a leaching-precipitation-calcination process. The effect of leaching parameters, such as H_2SO_4 acid concentration (C), temperature (T), time (t), solid/liquid ratio (S/L), and precipitation parameters: type of precipitating base (KOH, NaOH, NH_4OH), OH/Mg^{2+} ratio, and temperature on the obtained product properties, were investigated using Taguchi approach. The optimal leaching conditions were selected as: $C=5M$, $T=65\text{ }^\circ C$, $t=15\text{ min}$, and $S/L\text{ ratio}=1:5$. Furthermore, the potassium hydroxide (KOH) was selected as the optimal precipitating base with $OH/Mg^{2+} = 10.5$. The calcination of the precipitates at $800\text{ }^\circ C$ during 2 h made it possible to produce a high purity MgO (~99.45 %) with a crystallite size of approximately 16.5 nm and particles in the form of agglomerated porous plates with a high SSA ($70.42\text{ m}^2/g$) which may be of interest for some applications, such as catalysts or supports.

Keywords: Dolomite; Acid leaching; Precipitation; $Mg(OH)_2$; MgO; Calcination

1. Introduction

Magnesium oxide (MgO) has an immensely important attractive characteristics: high melting point (~2800 °C) [1-4], good chemical resistance [4-6], low dielectric constant [7, 8], high electrical resistance [5], low thermal conductivity [6], and non-toxicity [9]. It is used in many application fields [10], such as in cement production [1, 4, 11, 12], refractories elaboration [4, 13], water purification [14], as an antibacterial material [7, 15], biomaterial [16], in pharmaceuticals and cosmetics [7], in paints [17, 18], superconductor materials [7], electronic and optical components and catalysts [2, 12, 19, 20].

Magnesium oxide MgO is not available in nature. Therefore, it is produced from different mater sources. Seawater, natural magnesite $MgCO_3$, and dolomite $MgCa(CO_3)_2$ are the main candidate sources [1, 12, 21-24]. Seawater contains about 1.3 g/L of Mg, and the pure magnesium chloride solution could be obtained by removing impurities, which is usually complex operation and too expensive in terms of energy consumption [1]. The production of MgO from magnesite is usually carried out by thermal decomposition [25] or dissolving in acidic solution followed by precipitation with appropriate bases, and

finished by calcination [24]. Magnesite ores are geographically limited to a few countries such as Russia, China, Slovakia, Australia, Greece, Turkey, and Brazil [26]. In contrast, dolomite ores have larger deposits that are more widely distributed than that of magnesite [27]. For this reason, much attention has been paid to the use of dolomite as a favorable source to produce magnesia [28-31]. Altiner et al. [28] investigated the effect of leaching parameters of dolomite in HCl solution on the dissolution rate. In a follow-up study [8], periclase MgO nanoparticles with very interesting properties were produced from dolomite ore through pyrohydrolysis–calcination processes. The reactivity and particle size were found mainly influenced by the production temperature. The synthesized MgO particles size ranged from 180.05 nm to 6 μm . Furthermore, Altiner [29] investigated the effect of the base type used during the precipitation stage (NaOH, KOH, and NH_4OH) and the calcination temperature on the properties of synthesized MgO. The obtained MgO powders produced via the addition of NaOH exhibited the best properties, such as higher SSA ($44.547\text{ m}^2/g$) compared to those obtained with KOH ($34.282\text{ m}^2/g$) and NH_4OH ($21.336\text{ m}^2/g$).

In Algeria, there are several deposits rich in dolomite including that of Djebel Teioualt located in

*Corresponding author: kolmus_eulma@yahoo.fr



the territory of Ouled Hamla Municipality, Oum El Bouaghi State [18]. According to the Algerian Ministry of Energy and Mining, the geological reserve of dolomite in Teioualt massive is approximately 18 million tons [18]. With a good chemical composition in MgO and CaO (MgO~19.4 % and CaO~30 %) and low amount of impurities (~0.8%), this dolomite exhibits a particular interest for use in many fields and particularly in producing MgO.

In this work, Teioualt dolomite was used to synthesize pure MgO powders by leaching in an H₂SO₄ solution followed by precipitation and calcination. Despite its high cost compared to HCl and HNO₃ acids, sulfuric acid H₂SO₄ shows a good selective dissolution, where the majority of impurities will be combined with sulfate ions to form solid particles that can be separated easily from the solution by filtration [32]. Consequently, the obtained filtrate (Mg-rich solution) contains less amounts of Ca, Fe and Al impurities. Since the properties of the synthesized MgO are significantly affected by the synthesis conditions, the effect of leaching conditions (acid concentration, temperature, time, solid/liquid ratio) on dissolution efficiency was investigated based on the Taguchi approach.

In the precipitation stage, different bases were used to designate the appropriate one in terms of precipitation efficiency that will be used in the rest of the work. The Taguchi approach was reused to optimize the precipitation temperature and OH⁻/Mg²⁺ ratio. The precipitated magnesium hydroxide Mg(OH)₂ was transformed to magnesium oxide by calcination and all powders, before and after calcination, were subjected to physicochemical characterization (X-ray Fluorescence (XRF), X-ray diffraction (XRD), scanning electron microscopy (SEM), particle size Laser granulometry...).

2. Material and methods

2.1. Material

In this work, a raw dolomite ore (~1 mm) was taken from the Teioualt unit, the unique industrial dolomite production unit in Algerian territory. This dolomite is extracted from Teioualt quarry, Aïn M'lila/ Oum-El-Bouaghi, located in eastern Algeria. To obtain a representative sample from the used dolomite ore, a sampling was carried out by adopting coning and quartering method. The mean chemical composition determined by X-ray fluorescence (XRF, Rigaku ZSX Primus IV) is listed in Table 1. From chemical composition point of view, it appeared that

CaO/MgO ratio (CaO/MgO = 1.54) was quite acceptable compared with other dolomites, such as Nigerian dolomite which had CaO/MgO equal to 1.37 [33], Vietnam's dolomite 1.43 [34], Turkish dolomite 1.41 [28], China's dolomite 1.57 [27], and Egyptian dolomite 1.76 [35]. The presence of some impurities with low amounts not exceeding 0.8% in weight in totality was noticed, of which the most significant were SiO₂ (0.4 %), Al₂O₃ (0.23 %), and Fe₂O₃ (0.11 %).

The crystallographic composition of the raw material was determined by means of a Panalytical X'Pert Pro X-ray diffractometer (XRD) with Cu_{Kα} (λ=1.54 Å) radiation in the 2θ range of 10–80 ° with a 0.02 step angle. The diffraction data was evaluated using a Highscore Plus software program for mineral identification. From obtained pattern (Fig. 1(a)), it can be seen that the sample used in this study was mainly composed of dolomite mineral (CaMg(CO₃)₂-JCPDS: 96-900-3522) associated with a minor quantity of calcite (CaCO₃-JCPDS: 96-900-9668).

Fig. 1(b) shows the particle size distribution of the crushed dolomite determined using a Malvern Mastersizer 3000 H. The particle size distribution was in the form of a more or less symmetrical inverted bell. The maximum particle size was about d_{max} = 1160 μm and only a few amount of the particles were larger than 1 mm in size (~ 0.5 %). The d50 and d80 values deduced from the cumulative particle size at 50 % and at 80 % of the total volume were found equal to 190 and 475 μm, respectively.

The thermal behavior of the dolomite sample was investigated by DT/TG analysis using a DTA/TGA machine (TA instrument SDTQ600) on a crushed dolomite sample (~1g), with a heating rate of 10 °C.min⁻¹ up to T= 1000 °C. From the obtained curves (Fig. 1(c)), the unique thermal event that could be noted in the temperature range (23 °C-1000 °C) was endothermic that was maximum at 760 °C. This event was associated with a significant mass loss (~49.15 %) as observed on the TGA curve. The recorded mass loss corresponded to the full decomposition of the dolomite CaMg(CO₃)₂ to magnesia MgO and lime CaO on one step as follows (Eq. 1):



In the literature [36, 37], it was well established that some test conditions, such as small testing samples or atmosphere, gave rise to a unique DTA peak involving the decomposition of both carbonates in the same temperature range.

Table 1. Chemical composition of the Teioualt dolomite

Oxide	MgO	CaO	Al ₂ O ₃	SiO ₂	Fe ₂ O ₃	SO ₃	SrO	Cl	P ₂ O ₅	LOI
wt. (%)	19.42	29.97	0.23	0.40	0.11	0.04	0.008	0.005	0.015	49.8



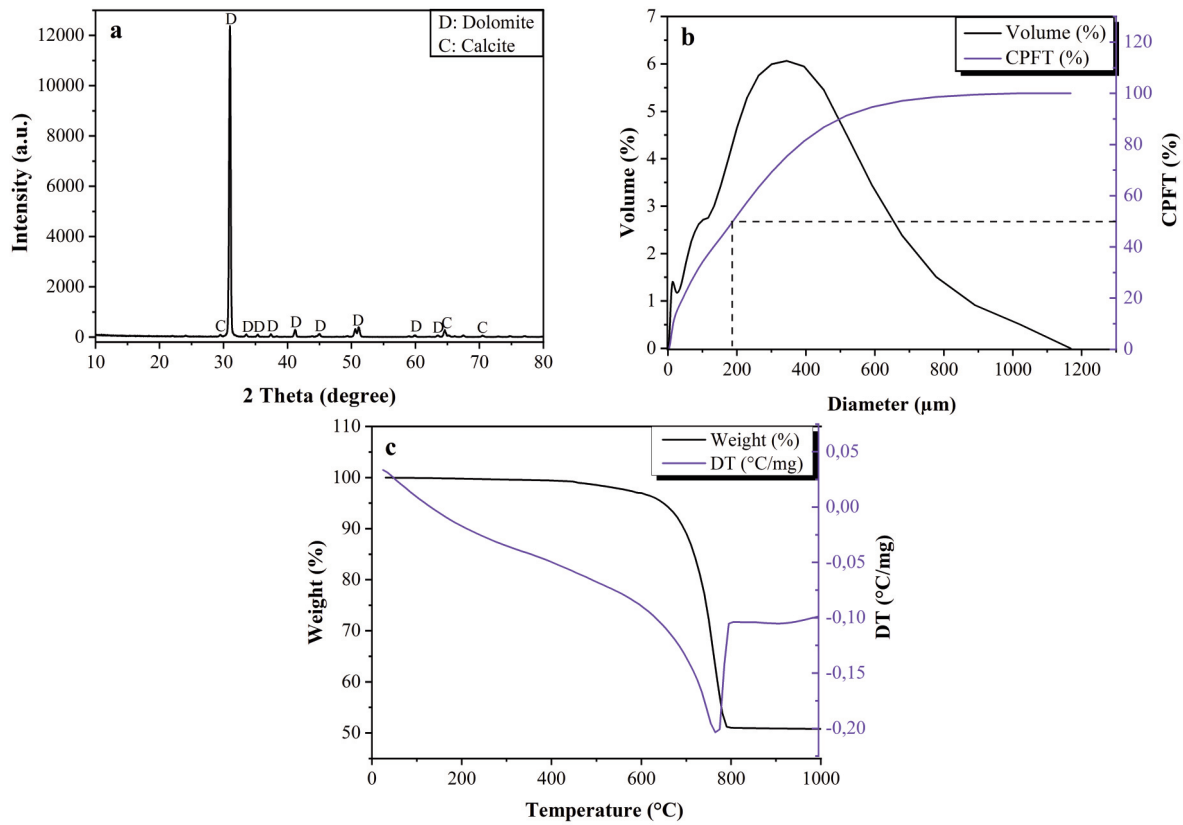


Figure 1. (a) XRD pattern (b) Particle size distribution and (c) DTA/TGA curves of the sample used in this study

2.2. Experimental process

2.2.1. Leaching

The experimental process followed in the production of MgO from the Teioualt dolomite ore, shown in Fig. 2, was divided into three main stages that included leaching, precipitation, and calcination. These three experimental stages were explained in detail in the following sub-sections.

The leaching tests were performed in a 250 mL three-necked jacketed reactor equipped with a hot water circulator (JSR) to provide the required reaction temperature. Furthermore, a glass spiral-type reflux condenser was added to the reactor in order to minimize the evaporation. The reaction temperature was controlled by an infrared thermometer (K-type, CEM, DT8835) and the pH solution was measured instantaneously by a pH meter (WTW 3110). The stirring of the solution was provided by a magnetic stirrer (MTOPS MS300HS). When the desired temperature was obtained, a predetermined amount of the sample was poured into the solution.

The effect of leaching parameters on the dissolution of Mg from the ore in the presence of H₂SO₄ was investigated based on the Taguchi approach providing satisfactory results with a minimum number of the experiments. The chemical reaction occurring between H₂SO₄ acid and dolomite can be schematized as follows (Eq. 2). The experimental conditions that were studied to dissolve Mg from the ore are listed in Table 2.

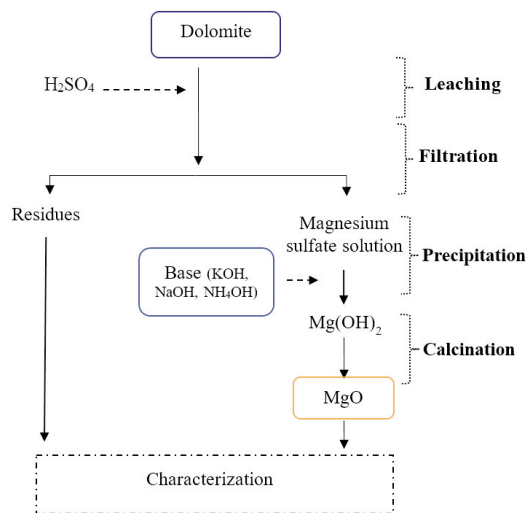
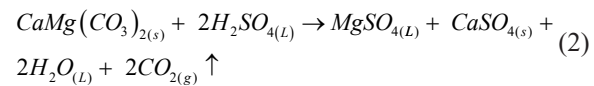


Figure 2. Flowchart of the followed experimental procedures



Table 2. Different conditions investigated in the leaching process according to the Taguchi approach

Conditions	Levels
Temperature (°C)	20, 35, 50, 65
Time (min)	30, 45, 60, 75
Molarity (M)	1, 3, 5, 7
Solid/Liquid ratio	1:4, 1:5, 1:6, 1:8

When the reaction time was reached, the solution was filtered using a vacuum pump and the residues were washed with hot pure water 3 times and dried at 100 °C for 24 h. The leachate solution was characterized by Atomic Absorption Spectroscopy (AAS, Perkin Elmer 900H) to quantify the amounts of dissolved Mg ions and other chemical elements identified as impurities. The Mg dissolution rate (MDR) was calculated using the following equation:

$$MDR (\%) = 100 \cdot (X_1 - X_2) / X_1 \quad (3)$$

Where:

X_1 (g): MgO mass in the initial sample.

X_2 (g): MgO mass in the residue obtained after leaching.

According to the amount of the dissolved Mg ions the most appropriate dissolution conditions were selected and applied in the rest of the work (precipitation stage).

In order to investigate the leaching reaction kinetics, an additional experimental tests were performed through the monitoring of the released CO₂ volume over time. For the leaching temperatures T=35, 50, and 65 °C and acid concentration (5 M), the test was carried out until complete reaction was reached, i.e., the released CO₂ rate was saturated. In all tests, the S/L ratio was kept constant and equal to 1:5. The amount of CO₂ released was calculated as follows:

$$CO_2 (\%) = 100 \cdot n \cdot MCO_2 / m \cdot X \quad (4)$$

Where:

n: is the mole's number of CO₂ that exists in the tank (cylindrical shape) given by:

$$n = Vg / 22400 \quad (5)$$

Vg: the volume occupied by the gas

M CO₂: the molar mass of CO₂ (g/mol)

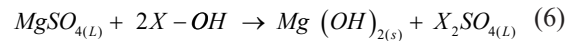
m: the weight of the sample used in the test (g)

X: the amount of CO₂ in the dolomite (%)

2.2.2. Precipitation

The Mg-rich sulfate solution obtained in the

leaching stage was used as starting solution in the precipitation tests. A volume of 100 mL was mixed with 100 mL pure water, then the used base was added to the mixture: sodium hydroxide [NaOH] (0.5 M, 300 mL), potassium hydroxide [KOH] (0.5 M, 300 mL) or ammonia [NH₄OH] (6.45 M, 650 mL). The occurring precipitation reaction can be described by Eq. 6.



Where, X is the Na⁺, K⁺ or NH₄⁺ based chemicals.

For each used base, the precipitation recovery (PR %) was calculated according to the following equation:

$$PR (\%) = 100 \cdot X_2 / X_1 \quad (7)$$

X_1 (g): the amount of Mg in the Mg sulfate solution used.

X_2 (g): the amount of Mg in the precipitate.

In the precipitation stage with KOH, the influence of the two precipitation test parameters: temperature (20, 35, 50, 65 °C) and hydroxyl to Mg molar ratio (OH⁻/Mg²⁺= 8, 9.5, 10.5, 12) on the precipitation rate of Mg(OH)₂ was investigated. The precipitation tests were carried out as follows: Mg-sulfate solution with a volume of 100 mL was poured in a 100 mL pure water. After that, the used base (V=300 mL) was gradually added to the mixture under constant stirring conditions (250 rpm) and maintained for 2 h at a fixed test temperature. The solution was aged for 24 h, filtered, washed 3 times with hot pure water, and dried at 100 °C for 24 h. The best precipitation conditions were selected according to the AAS results of the solution and chemical composition analysis of precipitates.

2.2.3. Calcination

The thermal behavior of the obtained precipitates was investigated using a TG/TD analysis (Mettler Toledo TGA 3+TA instrument SDTQ600) with a heating rate of 10 °C.min⁻¹ to optimize calcination conditions. Next, the precipitates were calcined at different temperatures and subjected to X-ray diffraction (XRD Rigaku Miniflex II and Bruker D8 Discover, Panalytical X'Pert Pro) using the Cu_{Kα} radiation (λ=1.54060 Å) in the 2θ range of 5 to 85° with a 0.02 step angle to identify developed crystalline phases (PDXL software). Fourier transform infrared spectroscopy (FTIR-Perkin Elmer) was performed in the wave number range 400–4000 cm⁻¹ and used to investigate calcination consequences. SEM-EDX (SEM, FEI, Quanta 650, and Zeiss Gemini) examinations were carried out to observe and analyze particles, and laser granulometry



(Malvern Mastersizer 300H) to determine the particle size distribution. The specific surface area was measured from the nitrogen adsorption/desorption at 77K using the Brunauer–Emmett–Teller (BET) method (Surfer, ThermoFisher Scientific).

The chemical composition of the dolomite ore was determined by X-ray fluorescence (XRF, Panalytical MiniPal 4). The concentrations of some ions such as Ca^{2+} , K^{+} in the leaching solutions were determined by AAS. In addition, a wet chemical analysis (EDTA titration) was performed to determine the chemical composition of the precipitates.

3. Results and discussion

3.1. Leaching

The MDR was measured for each test as described in the experimental procedure (section 2.2.1) and the obtained results are presented in Table 3. It appeared that each leaching parameter affected significantly the reaction kinetics, as shown by the evolution of MDR, which was consistent with many previous research works [28, 30, 33, 38-40]. The highest MDR (97.26 %) was obtained after leaching dolomite in the presence of H_2SO_4 (7M) at 65 °C for 1 h (Test L16), followed by 95.93 % of MDR when the dolomite was leached in H_2SO_4 (5 M) at 65 °C for 30 min (Test L12). The high amount of MDR ment that the reaction between dolomite and sulfuric acid, formulated in Eq. 3, was well accomplished. This finding was confirmed by the chemical composition of residues

Table 3. The amount of dissolved Mg (%) during leaching tests

Test	Molarity	Temperature (°C)	S/L ratio	Time (min)	Dissolved Mg (%)
L1	1	20	1:04	30	79.96
L2	1	35	1:05	45	89.56
L3	1	50	1:06	60	89.09
L4	1	65	1:08	75	92.37
L5	3	20	1:05	60	91.66
L6	3	35	1:04	75	94.26
L7	3	50	1:08	30	91.90
L8	3	65	1:06	45	94.08
L9	5	20	1:06	75	91.87
L10	5	35	1:08	60	94.80
L11	5	50	1:04	45	93.69
L12	5	65	1:05	30	95.93
L13	7	20	1:08	45	90.07
L14	7	35	1:06	30	94.32
L15	7	50	1:05	75	94.73
L16	7	65	1:04	60	97.26

obtained in the two optimal tests: L12 and L16 (see Table 4), which showed low percentage of not dissolved MgO. Considering these two optimal tests (L12 and L16), the obtained results were very close and for L16 test a more concentrated solution (7 M instead of 5 M for L12) was used during a double leaching time (60 min instead of 30 min for L12), the test L12 was selected for the rest of this work. Moreover, considering the amount of remaining impurities (mainly Fe_2O_3 and SiO_2 oxides) in the residues, it resulted that the L12 test led to more pure dissolved dolomite than that of the L16 test.

The signal-to-noise ratio (S/N) deduced from Taguchi's approach giving the simulation of the influence of the investigated conditions is shown in Fig. 3. It can be seen that reaction temperature showed the highest S/N ratio value, suggesting that reaction temperature was the more influential condition, followed by acid concentration, time, and finally by the solid to liquid ratio (S/L). The contribution of leaching conditions was found in the following order: Temperature (58.02 %) > Acid concentration (38.16 %) > Time (1.2 %) > S/L ratio (0.88 %).

Fig. 4 shows the CO_2 released according to the time for the temperatures 35, 50, and 65 °C. The plotted curves indicate that the dolomite dissolution rate increased with time and reached a plateau after a sufficient time that depended on temperature. For example, the complete dolomite dissolution (~100 % of released CO_2) was achieved after 40 min at 50 °C and only after 15 min at 65 °C. We concluded that leaching temperature accelerated the reaction kinetics, i.e., the same dissolution rate obtained at a defined

Table 4. Chemical composition of the residues obtained after leaching tests L12 and L16

Test	Composition (%)				
	CaO	MgO	Fe_2O_3	SiO_2	SO_3
L12	43.85	1.06	0.16	0.59	42.64
L16	49.40	0.88	0.066	0.4	46.78

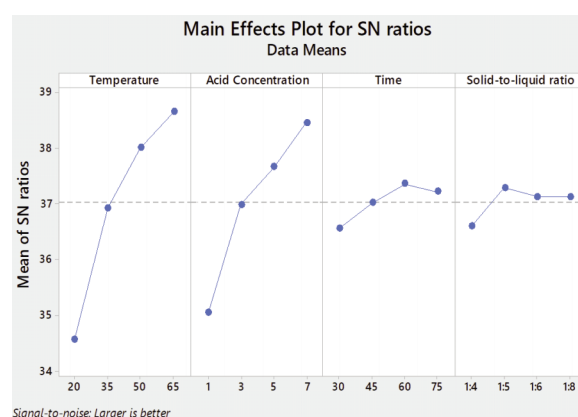


Figure 3. S/N Ratios for investigated conditions: Temperature, concentration, time and S/L ratio



temperature and time could be achieved at a higher temperature in a shorter time. In fact, lower temperatures increased viscosity and thus decreased reactant ion mobility, and so the lower reaction efficiencies were expected [31, 35]. Higher temperatures led to an increase in the efficiency of H_2SO_4 and consequently, higher leaching rate could be recorded. From the obtained results, the optimum selected temperature and time were 65 °C and 15 min, respectively.

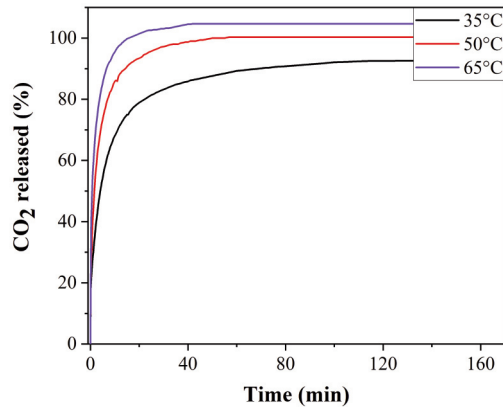


Figure 4. The amount of CO_2 released over time for different test temperatures ($C=5M$, $S/L=1:5$)

3.2. Precipitation

The leachate solution previously prepared according to the following leaching conditions ($C=5M$, $T=65^\circ C$, $t=15$ min, and S/L ratio = 1:5) was used in the precipitation stage. The elemental composition of the prepared leachate solution carried out by AAS was presented in Table 5. It is clear that the main constituent was magnesium with a percentage of 98.6% and that remaining impurities were Ca (1.32%), Fe (0.06%), and Al (0.03%).

Table 5. AAS of leachate solution used in the precipitation stage

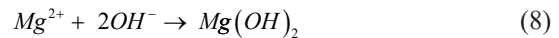
Elements	Mg	Ca	Fe	Al	Si
Amount (mg/L)	22356	298.7	13.84	7.048	< 5

In the precipitation stage, three alkaline bases were used (NaOH, KOH, and NH_4OH) and to select the best precipitating base, the magnesium precipitation recovery (PR) was calculated for each base. The obtained results (Table 6) showed that the highest precipitation recovery (PR) was obtained by KOH (67.41%), followed by NH_4OH and NaOH having almost the same PR values (60.96% and 60.42%). The KOH base and relative to the other ones can be considered as a very strong base because with this one it was possible to very effectively raise the pH of the solution to the desired values.

Table 6. Precipitation recovery PR for the three used bases

Base	KOH	NaOH	NH_4OH
PR (%)	67.41	60.42	60.96

Afterward, and for the best base (KOH), the effect of the temperature and OH^-/Mg^{2+} ratio on the Mg precipitation recovery was investigated using the Taguchi approach, and the results were listed in Table 7. Theoretically, to form one mole of $Mg(OH)_2$, each mole of Mg^{2+} required two moles of OH^- which resulted in an OH^-/Mg^{2+} ratio equal to 2 (see Eq. 8). Experimentally, it was observed that precipitation of $Mg(OH)_2$ particles started only when the OH^-/Mg^{2+} ratio reached 8 corresponding to measured pH~9. The supersaturation with OH^- species was experimentally necessary and allowed the formation of clusters with a very low size (r_0) which increased to form a critical nucleus ($r>r_0$). Then the crystal grew gradually and formed bigger one ($r>>r_0$) [38]. Another effect was that an increase in the OH^-/Mg^{2+} ratio led to an increase in the pH value which made the precipitated $Mg(OH)_2$ particles more stable [39].



With increasing the OH^-/Mg^{2+} ratio, a significant increase in PR values was recorded and regardless of the temperature, the complete recovery (PR=100%) was achieved at OH^-/Mg^{2+} ratio equal to 10.5. For OH^-/Mg^{2+} ratios lower than 10.5, no significant changes were noted if temperature varied. From Taguchi approach, the contribution OH^-/Mg^{2+} (99.42%) to the precipitation result was found more significant than temperature (0.58%).

In order to improve purity, an additional purification step was carried out by removing $Fe(OH)_3$ using KOH base. Firstly, the KOH base was added slowly to the Mg-rich solution until the pH value ranged between 4.5 and 5.5 at which the $Fe(OH)_3$ particles were formed and could be separated from the solution by filtration. After that, the remaining KOH solution was added completely to the Mg-rich solution to form $Mg(OH)_2$ particles that were then filtered, washed with hot pure water, and dried at 80 °C for 24 h.

The thermal behavior of the obtained precipitates was followed by DSC/TG analysis and the obtained curves are presented in Fig. 5. A total mass loss of about 31.3% constituted of two distinguished parts: the first one of about 2% occurred between room temperature and 200 °C and was caused by the release of adsorbed water. The second one of approximately 29.3%, took place simultaneously with an important exothermic event taking its maximum at $T=400^\circ C$. This was attributed to the decomposition of $Mg(OH)_2$ to MgO and H_2O according to the equation 9 which suggested a theoretical mass loss of good agreement

with the recorded one (~31 %wt.) and with previous published works [17, 40, 41]. We also note that the deshydroxylation continued above 400 °C but very slowly.

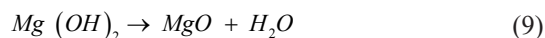


Table 7. Mg precipitation recovery PR (%) under different temperatures and Mg/OH ratios

Test	Conditions		Mg recovery (%)
	Temperature (°C)	OH/Mg ²⁺ ratio	
P1	20	8	53.05
P2	20	9.5	84.29
P3	20	10.5	100
P4	20	12	100
P5	35	8	52.89
P6	35	9.5	78.28
P7	35	10.5	100
P8	35	12	100
P9	50	8	53.51
P10	50	9.5	90.91
P11	50	10.5	100
P12	50	12	100
P13	65	8	53.03
P14	65	9.5	92.21
P15	65	10.5	100
P16	65	12	100

The precipitated Mg(OH)₂ was calcined at different temperatures (400, 600, 800 °C) for 2h and analyzed by XRD. The obtained patterns (Fig. 6) showed clearly the evolution of the precipitates from hydrated state Mg(OH)₂ (JCPDS 00-007-0239) before calcination to perfectly anhydrous state MgO (JCPDS 01-089-7746) after calcination at 800 °C for 2 h. The calcination at temperatures lower than 800 °C resulted in a mixture of Mg(OH)₂ and MgO, as was revealed by the coexistence of their peaks. From these results, it was assumed that calcination at a temperature of 800 °C was sufficient to produce MgO particles from the precipitated Mg(OH)₂.

Non-calcined precipitates (23 °C) and those calcined at 800 °C for 2 h were subjected to FTIR spectroscopy and the obtained spectra are presented in Fig. 7. For not calcined precipitates, the strong band at 3693 cm⁻¹ was attributed to stretching vibration of the hydroxyl band (O-H) in the crystal structure of Mg(OH)₂ [42-45]. An overlaying bands in the range of 1410-1560 cm⁻¹ resulted from the stretching vibration mode of the surface hydroxyl group [42, 43, 46] and

the deformation vibration of Mg-O-Mg [47]. A weak band was observed at 856 cm⁻¹ referring to Mg-O-Mg bonds [48, 49]. After calcination at 800 °C, the hydroxyl band (O-H) in the crystal structure of Mg(OH)₂ disappeared completely which proved that the complete decomposition of Mg(OH)₂ and its transformation to MgO was good, as was already

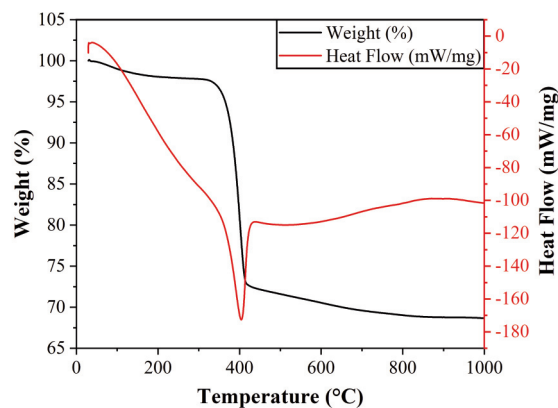


Figure 5. TGA-DSC curves of Mg(OH)₂ precipitated and purified by KOH base

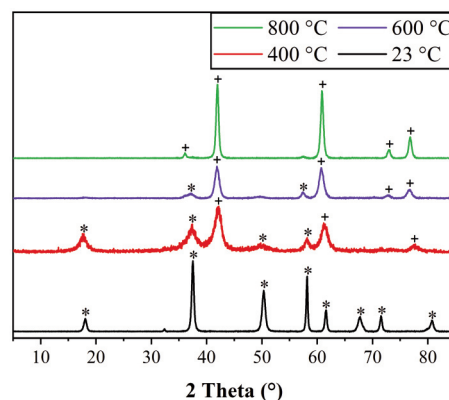


Figure 6. XRD patterns of Mg(OH)₂ precipitated by KOH and calcined at different temperatures for 2h: (*) Mg(OH)₂, (+) MgO

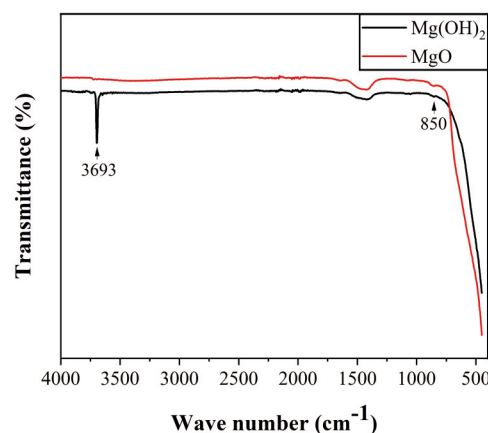


Figure 7. FTIR curves of precipitated Mg(OH)₂ before and after calcination at 800 °C for 2h

confirmed by the XRD results (see Fig. 6).

The synthesized MgO powders exhibited a purity of about 99.45 % and the major remaining impurities were Fe_2O_3 (0.01 %), CaO (0.39 %) derived from dolomite and K_2O (0.15 %) derived from KOH used as precipitating base.

The followed process led to $\text{Mg}(\text{OH})_2$ agglomerated hexagonal nanoplates of approximately 50 nm in diagonal and 10 nm in thickness (Fig. 8(a)). A similar morphology was observed for $\text{Mg}(\text{OH})_2$ synthesized by different ways [40, 43, 48].

The calcination of $\text{Mg}(\text{OH})_2$ at 800 °C for 2 h resulted in a particular MgO morphology (Fig. 8(b)) that consisted of rounded porous plates. It was likely that the observed porosity resulted from the release of structural water of $\text{Mg}(\text{OH})_2$ after calcination, according to the equation 9. In previous research [41, 50-52], many other morphologies were found, such as rods, flowers, flakes, spheres, and hexagonal plates depending on the used process, the precursors and preparation conditions.

The N_2 adsorption/desorption profiles for the synthesized MgO are presented in Fig.9. According to the IUPAC classification the N_2 isotherm was a type III isotherm with a type H_3 hysteresis loop. This type of hysteresis is usually found on solids consisting of aggregates or agglomerates of particles forming pores, with a nonuniform size and/or shape [17, 19, 53]. The synthesized MgO powder exhibited a high SSA of 70.42 m^2/g . According to Jin et al. categorization [54], MgO with SSA more than 60

m^2/g is classified in “category I” which refers to high reactive magnesium oxide [12, 54]. The SSA of the synthesized MgO was judged good compared to some other works [12, 29, 54] and it made possible its use in a variety of applications that required a high SSA, such as catalysts or supports.

As can be seen from Fig. 8, the developed plates were in agglomeration state that led to a micrometric particle size. The particle size with a d_{50} value of 50.8 and 60.3 μm was recorded for $\text{Mg}(\text{OH})_2$ and MgO, respectively, whereas the maximum particle size was found approximately the same, $d_{\text{max}} = 666 \mu\text{m}$.

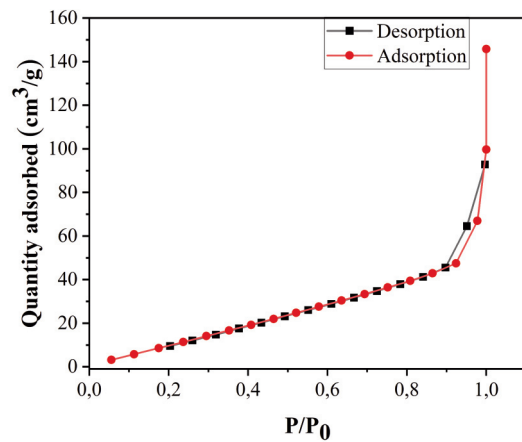


Figure 9. N_2 adsorption/desorption isotherms of the MgO synthesized

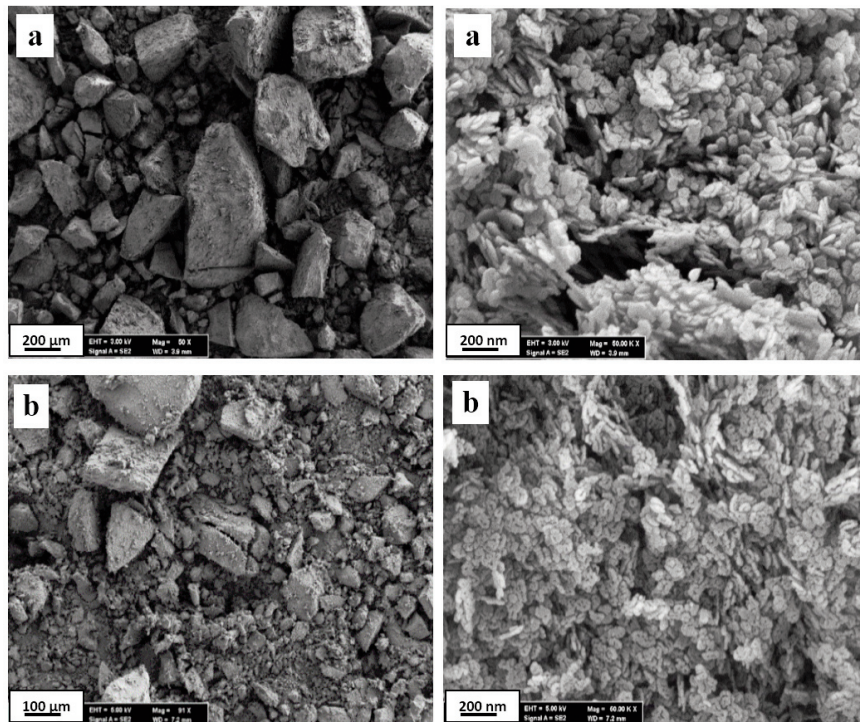


Figure 8. SEM observations of synthesized (a) $\text{Mg}(\text{OH})_2$ and (b) MgO powders

The crystallite size (d) of the developed MgO particles was calculated from the XRD spectra (Fig. 6) by Scherrer's law (Eq. 10):

$$d = K \cdot \lambda / \beta \cdot \cos\theta \quad (10)$$

where: K- form factor (~ 0.89); λ - wavelength of the X-rays used ($\lambda = 0.15406$ nm); β - Full width at half maximum (FWHM) of the most intense peak (in Radians) given by (002) plane; and θ - Bragg angle of the considered peak.

The calculated crystallite size for the synthesized MgO was found to be approximately $d=16.5$ nm which was well comparable to the values found by Kumar et al. [55, 56] ranging between 3 and 73.5 nm, and that obtained by Meshkani varying between 12.2 and 14.2 nm [45] using precipitation method.

For the optimal investigated conditions, the recovery rate of MgO (R) was calculated according to the following relationship:

$$R(\%) = \frac{m_2}{m_1} \cdot 100(\%) \quad (11)$$

Where: m_2 and m_1 are MgO mass in the synthesized powder and in the dolomite ore, respectively.

In this work, a recovery rate (R) equal to 97.2 % was recorded, which constituted a very good result in comparison with some similar works [31, 35, 43].

4. Conclusion

In this paper, by using the Algerian dolomite ore as raw material, a high purity (~ 99.45 %) nanometric $\text{Mg}(\text{OH})_2$ and MgO crystals were well synthesized using leaching with H_2SO_4 , followed by precipitation by KOH, then calcination. The best synthesizing conditions were found to be: leaching by H_2SO_4 acid solution (5 M) during 15 min at a reaction temperature 65 °C with a solid to liquid ratio 1:5 and precipitation with KOH base with an OH/Mg^{2+} ratio of 10.5. The calcination at the temperature $T=800$ °C, appeared to be sufficient to transform all precipitated hydrate magnesium oxide $\text{Mg}(\text{OH})_2$ to anhydrous magnesium oxide MgO, as was demonstrated by the XRD and TGA/TDA results. The SEM observations showed that precipitated $\text{Mg}(\text{OH})_2$ appeared in the form of agglomerated hexagonal nanoplates of approximately 50 nm in diagonal and 10 nm in thickness and that its calcination at 800 °C for 2 hours resulted in a particular MgO rounded porous plates with a high SSA (70.42 m^2/g) that could be attractive for some applications such as catalysts or supports. The recovery rate (R) recorded for the optimal investigated conditions of the used process was found to be 97.2 %.

Acknowledgements

This study was supported by DGRSDT (Algeria) and Çukurova University (Turkey).

Author's contributions

Chafia Boucekrit: Performed the experiments tests, Formal analysis, discussed the results, and wrote the original draft. Mostafa Kolli: Discussed the results, and reviewed the original draft; Mahmut Altiner: Formal analysis, reviewed the original draft; Rachida Doufnoune: Formal analysis, reviewed the original draft;

Conflict of interest statement

The authors declare that they have no known competing financial interests or personal relationships that could have appeared to influence the work reported in this paper.

References

- [1] J. H. Canterford, Magnesia-An important industrial mineral: A review of processing options and uses, *Mineral Processing and Extractive Metallurgy Review*, 2 (1-2) (1985) 57–104. <https://doi.org/10.1080/08827508508952601>
- [2] Y. Yin, G. Zhang, Y. Xia, Synthesis and characterization of MgO nanowires through a vapor-phase precursor method, *Advanced Functional Materials*, 12 (4) (2002) 293-298. [https://doi.org/10.1002/1616-3028\(20020418\)12:4<293::AID-ADFM293>3.0.CO;2-U](https://doi.org/10.1002/1616-3028(20020418)12:4<293::AID-ADFM293>3.0.CO;2-U)
- [3] C. Sadik, O. Moudeden, A. El Bouari, I.-E. El Amrani, Review on the elaboration and characterization of ceramics refractories based on magnesite and dolomite, *Journal of Asian Ceramic Societies*, 4 (3) (2016) 219–233. <https://doi.org/10.1016/j.jascer.2016.06.006>
- [4] Y. Cui, D. Qu, X. Luo, X. Liu, Y. Guo, Effect of La_2O_3 addition on the microstructural evolution and thermomechanical property of sintered low-grade magnesite, *Ceramics International*, 47 (3) (2021) 3136–3141. <https://doi.org/10.1016/j.ceramint.2020.09.150>
- [5] S. Lei, Y. Gan, Z. Cao, S. Wang, H. Zhong, The preparation of high purity MgO and precision separation mechanism of Mg and Ca from dolomite, *Mining & Metallurgy Exploration*, 37 (2020) 1221–1230. <https://doi.org/10.1007/s42461-020-00213-w>
- [6] D. Feng, X. Luo, G. Zhang, Z. Xie, P. Han, Effect of Al_2O_3 + 4SiO_2 additives on sintering behavior and thermal shock resistance of MgO-based ceramics, *Refractories and Industrial Ceramics*, 57 (2016) 417–422. <https://doi.org/10.17073/1683-4518-2016-8-48-54>
- [7] S. S. Mirtalebi, H. Almasi, M. A. Khaledabad, Physical, morphological, antimicrobial and release properties of novel MgO-bacterial cellulose nanohybrids prepared by in-situ and ex-situ methods, *International Journal of Biological Macromolecules*,



- 128 (2019) 848–857.
<https://doi.org/10.1016/j.ijbiomac.2019.02.007>
- [8] M. Altiner, M. Yildirim, Preparation of periclase (MgO) nanoparticles from dolomite by pyrohydrolysis–calcination processes, *Asia-Pacific Journal of Chemical Engineering*, 12 (6) (2017) 842–857. <https://doi.org/10.1002/apj.2123>
- [9] T. Ishikawa, K. Tsujikura, M. Tanaka, N. Nishida, A. Mitani, Morphological changes and their thermal conductivities of MgO crystals containing various impurities (B, Ca, Si), *International Journal of Applied Ceramic Technology*, 17 (6) (2020) 2734–2743. <https://doi.org/10.1111/ijac.13616>
- [10] A. Ranaivosoloarimanana, T. Quiniou, M. Meyer, F. Rocca, Analyse de la décomposition thermique de l'hydroxyde de magnésium, 11ème Inter-Congrès des Sciences du Pacifique et 2^{èmes} Assises de la Recherche française dans le Pacifique. Les Pays du Pacifique et leur environnement océanique face aux changements locaux et globaux, <https://hal.archives-ouvertes.fr/hal-03379435>.
- [11] S. Ruan, C. Unluer, Influence of mix design on the carbonation, mechanical properties and microstructure of reactive MgO cement-based concrete, *Cement and Concrete Composites*, 80 (2017) 104–114. <https://doi.org/10.1016/j.cemconcomp.2017.03.004>
- [12] H. Dong, C. Unluer, E.-H. Yang, A. Al-Tabbaa, Synthesis of reactive MgO from reject brine via the addition of NH₄OH, *Hydrometallurgy*, 169 (2017) 165–172. <https://doi.org/10.1016/j.hydromet.2017.01.010>
- [13] A. M. Amer, A contribution to hydrometallurgical processing of low-grade Egyptian dolomite deposits, *Hydrometallurgy*, 42 (3) (1996) 345–356. [https://doi.org/10.1016/0304-386X\(95\)00088-X](https://doi.org/10.1016/0304-386X(95)00088-X)
- [14] C. Xiong, W. Wang, F. Tan, F. Luo, J. Chen, X. Qiao, Investigation on the efficiency and mechanism of Cd (II) and Pb (II) removal from aqueous solutions using MgO nanoparticles, *Journal of Hazardous Materials*, 299 (2015) 664–674. <https://doi.org/10.1016/j.jhazmat.2015.08.008>
- [15] F. Al-Hazmi, F. Alnowaiser, A.A. Al-Ghamdi, A. A. Al-Ghamdi, M.M. Aly, R. M. Al-Tuwirqi, F. El-Tantawy, A new large-scale synthesis of magnesium oxide nanowires: structural and antibacterial properties, *Superlattices and Microstructures*, 52 (2) (2012) 200–209. <https://doi.org/10.1016/j.spmi.2012.04.013>
- [16] S. Sholicha, W. Setyarsih, G. Sabrina, L. Rohmawati, Preparation of CaCO₃/MgO from Bangkalan's dolomite for raw biomaterial, *IOP Conference Series: Journal of Physics: Conference Series*, 1171 (2019), 012034: IOP Publishing. <https://doi.org/10.1088/1742-6596/1171/1/012034>
- [17] I.F. Mironyuk, V.M. Gun'ko, M.O. Povazhnyak, V.I. Zarko, V.M. Chelyadin, R. Leboda, J. Skubiszewska-Zieba, W. Janusz, Magnesia formed on calcination of Mg(OH)₂ prepared from natural bischofite, *Applied Surface Science*, 252 (12) (2006) 4071–4082. <https://doi.org/10.1016/j.apsusc.2005.06.020>
- [18] K. Abdelaoui, D. Bedghiou, A. Boumaza, Comparative study of thermal and compositional properties of Ain M'lila dolomite, CaCO₃, and MgCO₃ using TG and FTIR analyses, *Journal of Advanced Research in science and Technology*, 7 (2020) 42–53.
- [19] T.H.Y. Duong, T.N. Nguyen, H.T. Oanh, T.A.D. Thi, L.N.T. Giang, H. T. Phuong, N.T. Anh, B.M. Nguyen, V.T. Quang, G.T. Le, T.V. Nguyen, Synthesis of magnesium oxide nanoplates and their application in nitrogen dioxide and sulfur dioxide adsorption, *Journal of Chemistry*, (2019) 4376429. <https://doi.org/10.1155/2019/4376429>
- [20] M.B. Nguyen, G.H. Le, T.T.T. Pham, G.T.T. Pham, T. T.T. Quan, T.D. Nguyen, T.A. Vu, Novel nano-Fe₂O₃-Co₃O₄ modified dolomite and its use as highly efficient catalyst in the ozonation of ammonium solution, *Journal of Nanomaterials*, (2020) 4593054. <https://doi.org/10.1155/2020/4593054>
- [21] R. Carson, J. Simandl, Kinetics of magnesium hydroxide precipitation from seawater using slaked dolomite, *Minerals Engineering*, 7 (4) (1994) 511–517. [https://doi.org/10.1016/0892-6875\(94\)90164-3](https://doi.org/10.1016/0892-6875(94)90164-3)
- [22] B. Petric, N. Petric, Investigations of the rate of sedimentation of magnesium hydroxide obtained from seawater, *Industrial Engineering Chemistry Process Design and Development*, 19 (3) (1980) 329–335. <https://doi.org/10.1021/i260075a001>
- [23] A. S. Bhatti, D. Dollimore, A. Dyer, Magnesia from seawater: a review, *Clay Minerals*, 19 (1984) 865–875. <https://doi.org/10.1180/claymin.1984.019.5.14>
- [24] A. Bhargava, J. A. Alarco, I. D. R. Mackinnon, D. Page, A. Ilyushechkin, Synthesis and characterisation of nanoscale magnesium oxide powders and their application in thick films of Bi,Sr₂CaCu₂O₈, *Materials Letters*, 34 (3-6) (1998) 133–142. [https://doi.org/10.1016/S0167-577X\(97\)00148-1](https://doi.org/10.1016/S0167-577X(97)00148-1)
- [25] V. S.S. Birchal, S.D.F. Rocha, V.S.T. Ciminelli, The effect of magnesite calcination conditions on magnesia hydration, *Minerals Engineering*, 13 (14-15) (2000) 1629–1633. [https://doi.org/10.1016/S0892-6875\(00\)00146-1](https://doi.org/10.1016/S0892-6875(00)00146-1)
- [26] Magnesite reserves worldwide as of 2020, by major countries, <https://www.statista.com/statistics/264953/global-reserves-of-magnesium-by-major-countries/>, 2021 (accessed April 2021).
- [27] J. Yu, J. Qian, F. Wang, Z. Li, X. Jia, Preparation and properties of a magnesium phosphate cement with dolomite, *Cement and Concrete Research*, 138 (2020) 106235 1–17. <https://doi.org/10.1016/j.cemconres.2020.106235>
- [28] M. Altiner, M. Yildirim, T. Yilmaz, Leaching of Mersin/aydincik dolomite ore in hydrochloric acid. Dissolution rates, *Physicochemical Problems of Mineral Processing*, 52 (2) (2016) 536–550. <https://doi.org/10.5277/ppmp160202>
- [29] M. Altiner, Effect of base types on the properties of MgO particles obtained from dolomite ore, *Mining, Metallurgy & Exploration*, 36 (2019) 1013–1020. <https://doi.org/10.1007/s42461-019-00122-7>
- [30] M. Yildirim, H. Akarsu, Preparation of magnesium oxide (MgO) from dolomite by leach-precipitation-pyrohydrolysis process, *Physicochemical Problems of Mineral Processing*, 44 (2010) 257–272.
- [31] E-S. A. Abdel-Aal, Possibility of utilizing Egyptian dolomite ores for production of magnesium oxide by acid leaching, *Fizykochemiczne Problemy Mineralurgii*, 29 (1995) 55–65.
- [32] M.F.R. Fouda, M.M. Abd-Elzاهر, R.S. Amin, Exploitation of Egyptian dolomite and magnesite ores for the preparation of magnesium compounds II. Kinetics of the reaction with nitric and sulphuric acids, *South African Tydskr Chemistry*, 52 (2/3) (1999)



- 90–94.
- [33] A.A. Baba, A.O. Omipidan, F.A. Adekola, O. Job, A. G.F. Alabi, A. Baral, R. Samal, Optimization study of a Nigerian dolomite ore dissolution by hydrochloric acid, *Journal of Chemical Technology and Metallurgy*, 49 (3) (2014) 280–287.
- [34] V.V. Quyen, V.T.T. Trang, N.D. Nam, T.D. Huy, D.N. Binh, Research on the manufacturing magnesium from thanhhoa dolomite by pigeon process, *Chemical Engineering*, «EUREKA: Physics and Engineering», 6 (2020) 97–107. <https://doi.org/10.21303/2461-4262.2020.001383>
- [35] M. Rashad, H. M. Baioumy, Chemical processing of dolomite associated with the phosphorites for production of magnesium sulfate heptahydrate, *The European Journal of Mineral Processing and Environmental Protection*, 5 (2) (2005) 174–183.
- [36] R. McIntosh, J. Sharp, F. W. Wilburn, The thermal decomposition of dolomite, *Thermochimica Acta*, 165 (2) (1990) 281–296. [https://doi.org/10.1016/0040-6031\(90\)80228-Q](https://doi.org/10.1016/0040-6031(90)80228-Q)
- [37] M. Samtani, D. Dollimore, F. W. Wilburn, K. Alexander, Isolation and identification of the intermediate and final products in the thermal decomposition of dolomite in an atmosphere of carbon dioxide, *Thermochimica Acta*, 367-368 (2001) 285–295. [https://doi.org/10.1016/S0040-6031\(00\)00662-6](https://doi.org/10.1016/S0040-6031(00)00662-6)
- [38] Q. Yuan, Z. Lu, P. Zhang, X. Luo, X. Ren, T. D. Golden, Study of the synthesis and crystallization kinetics of magnesium hydroxide, *Materials Chemistry and Physics*, 162 (2015) 734–742. <https://doi.org/10.1016/j.matchemphys.2015.06.048>
- [39] A. A. Pilarska, Ł. Klapiszewski, T. Jesionowski, Recent development in the synthesis, modification and application of Mg(OH)₂ and MgO: A review, *Powder Technology*, 319 (2017) 373–407. <https://doi.org/10.1016/j.powtec.2017.07.009>
- [40] G. Li, Z. Li, H. Ma, X. Jiang, W. Yao, Preparation of magnesia nanoballs from dolomite, *Integrated Ferroelectrics*, 145 (2013) 170–177. <https://doi.org/10.1080/10584587.2013.789301>
- [41] E. Alvarado, L. Torres-Martinez, A. Fuentes, P. Quintana, Preparation and characterization of MgO powders obtained from different magnesium salts and the mineral dolomite, *Polyhedron*, 19 (22-23) (2000) 2345–2351. [https://doi.org/10.1016/S0277-5387\(00\)00570-2](https://doi.org/10.1016/S0277-5387(00)00570-2)
- [42] M.M.M.G.P.G. Mantilaka, H.M.T.G.A. Pitawala, D.G.G.P. Karunaratne, R.M.G. Rajapakse, Nanocrystalline magnesium oxide from dolomite via poly (acrylate) stabilized magnesium hydroxide colloids, *Colloids and Surfaces A: Physicochemical and Engineering Aspects*, 443 (2014) 201–208. <https://doi.org/10.1016/j.colsurfa.2013.11.020>
- [43] Y. Xiong, B. Wu, J. Zhu, X. Fan, P. Cai, J. Wen, X. Liu, Preparation of magnesium hydroxide from leachate of dolomitic phosphate ore with dilute waste acid from titanium dioxide production, *Hydrometallurgy*, 142 (2014) 137–144. <https://doi.org/10.1016/j.hydromet.2013.11.013>
- [44] Q. Sun, B. Chen, X. Wu, M. Wang, C. Zhang, X-F. Zeng, J-X. Wang, J-F. Chen, Preparation of transparent suspension of lamellar magnesium hydroxide nanocrystals using a high-gravity reactive precipitation combined with surface modification, *Industrial & Engineering Chemistry Research*, 54 (2) (2015) 666–671. <https://doi.org/10.1021/ie504265z>
- [45] F. Meshkani, M. J. P. T. Rezaei, Facile synthesis of nanocrystalline magnesium oxide with high surface area, *Powder Technology*, 196 (1) (2009) 85–88. <https://doi.org/10.1016/j.powtec.2009.07.010>
- [46] S. Yousefi, B. Ghasemi, M. Tajally, A. Asghari, Optical properties of MgO and Mg(OH)₂ nanostructures synthesized by a chemical precipitation method using impure brine, *Journal of Alloys and Compounds*, 711 (2017) 521–529. <https://doi.org/10.1016/j.jallcom.2017.04.036>
- [47] S. Dai, Q. Wen, F. Huang, Y. Bao, X. Xi, Z. Liao, J. Shi, C. Ou, J. Qin, Preparation and application of MgO-loaded tobermorite to simultaneously remove nitrogen and phosphorus from wastewater, *Chemical Engineering Journal*, 446 (2022) 136809. <https://doi.org/10.1016/j.cej.2022.136809>
- [48] G. Balakrishnan, R. Velavan, K. M. Batoo, E. H. Raslan, Microstructure, optical and photocatalytic properties of MgO nanoparticles, *Results in Physics*, (2020) 16 103013 1-4. <https://doi.org/10.1016/j.rinp.2020.103013>
- [49] M. Kuang, Y. Shang, G. Yang, B. Liu, B. Yang, Facile synthesis of hollow mesoporous MgO spheres via spray-drying with improved adsorption capacity for Pb (II) and Cd (II), *Environmental Science and Pollution Research*, 26 (2019) 18825–18833. <https://doi.org/10.1007/s11356-019-05277-w>
- [50] Y. Zhang, M. Ma, X. Zhang, B. Wanga, R. Liu, Synthesis, characterization, and catalytic property of nanosized MgO flakes with different shapes, *Journal of Alloys and Compounds*, 590 (2014) 373–379. <https://doi.org/10.1016/j.jallcom.2013.12.113>
- [51] N. Sutradhar, A. Sinhamahapatra, S.K. Pahari, P. Pal, H.C. Bajaj, I. Mukhopadhyay, A.B. Panda, Controlled synthesis of different morphologies of MgO and their use as solid base catalysts, *Journal of Physical Chemistry C*, 115 (25) (2011) 12308–12316. <https://doi.org/10.1021/jp2022314>
- [52] M. Chinthala, A. Balakrishnan, P. Venkataraman, V. M. Gowtham, R. K. Polagani, Synthesis and applications of nano-MgO and composites for medicine, energy, and environmental remediation: a review, *Environmental Chemistry Letters*, 19 (2021) 4415–4454. <https://doi.org/10.1007/s10311-021-01299-4>
- [53] S. Melouki, Synthèse, caractérisation de charbons actifs fonctionnalisés et étude de leurs applications en élimination de polluants, PhD Thesis, Sciences Faculty, Mohamed Boudiaf University M'sila, Algeria (2021) p115.
- [54] F. Jin, A. Al-Tabbaa, Characterisation of different commercial reactive magnesia, *Journal of Advances in Cement Research*, 26 (2) (2014) 101–113. <https://doi.org/10.1680/adr.13.00004>
- [55] A. Kumar, J. Kumar, On the synthesis and optical absorption studies of nano-size magnesium oxide powder, *Journal of Physics and Chemistry of Solids*, 69 (11) (2008) 2764–2772. <https://doi.org/10.1016/j.jpcs.2008.06.143>
- [56] A. Kumar, S. Thota, S. Varma, J. Kumar, Sol-gel synthesis of highly luminescent magnesium oxide nanocrystallites, *Journal of Luminescence*, 131 (4) (2011) 640–648. <https://doi.org/10.1016/j.jlumin.2010.11.008>



SINTEZA MAGNEZITA MgO VISOKE ČISTOĆE IZ ALŽIRSKE DOLOMITNE RUDE

C. Boucekrit ^{a,b}, M. Kolli ^{a,b,*}, M. Altiner ^c, R. Doufnoune ^{a,d}

^a Univerzitet Ferhat Abas u Setifu, Odeljenje za istraživanje novih materijala, Setif, Alžir

^b Univerzitet Ferhat Abas u Setifu, Institut za optiku i preciznu mehaniku, Setif, Alžir

^c Çukurova univerzitet, Odsek za rudarstvo, Adan, Turska

^d Univerzitet Ferhat Abas u Setifu, Tehnološki fakultet, Setif, Alžir

Apstrakt

Nanometričke $Mg(OH)_2$ i MgO čestice visoke čistoće uspešno su sintetizovane iz alžirskog dolomita postupkom luženje-taloženje-kalcinacija. Uticaj parametra luženja, kao što su koncentracija kiseline H_2SO_4 (C), temperatura (T), vreme (t), odnos čvrsto-tečno (S/L) i parametra taloženja, kao što su vrsta taložne baze (KOH, NaOH, NH_4OH), OH/Mg²⁺ odnos i temperatura, na svojstva dobijenog proizvoda, ispitivani su pomoću Tagučijeve metodologije. Kao optimalni, izabrani su sledeći uslovi prilikom luženja: C=5M, T=65 °C, t=15 min i S/L odnos = 1:5. Pored toga, kalcijum hidroksid (KOH) je izabran kao optimalna taložna baza sa OH/Mg²⁺ = 10.5. Kalcinacija taloga na 800 °C tokom 2 sata omogućila je stvaranje MgO velike čistoće (~99.45 %) gde je veličina kristalita bila približno 16,5 nm, a čestice u obliku grozdastih poroznih ploča sa visokim SSA (70,42 m²/g), što može biti od interesa za neke primene, kao što su izrada katalizatora ili nosača.

Ključne reči: Dolomit; Kiselo luženje; Taloženje; $Mg(OH)_2$; MgO; Kalcinacija

